Wood Science and Technology 30 (1996) 307–321

Characterization of crack propagation in particleboard

R. J. A. Ehart, S. E. Stanzl-Tschegg, E. K. Tschegg

Summary In this paper the wedge-splitting-method (Tschegg 1986) for mode I-testing was applied to specimens of particleboard. Specimen geometry and loading-device used for this method allow testing under the condition of steady state crack propagation. Therefore the full load-displacement curves can be recorded. Using the load-displacement-curves, different ways of evaluation have been carried out to determine relevant fracture properties like the specific fracture energy G_f and the crack resistance R_C of the investigated material for two different orientations.

Introduction

Particleboard is a highly anisotropic heterogeneous material. Therefore application of LEFM's methods does not promise too much success. Two main mechanisms are involved in crack propagation. 1. Delamination in the crack tip process-zone (microcracking) and 2. Fiber bridging, which means that fibers bridge the crack in the wake behind the crack tip. These effects change the stress distribution around the crack tip in such a way that the stress singularity of LEFM is reduced by the process-zone and crack-closure forces can still be transmitted by fibers after the crack tip has passed.

Usual testing methods yield maximum values for the beginning of failure for various kinds of loading (3-point bending, CT, screw-pullout, . . .) like yield strength or fracture toughness (Niemz 1992), but little information about the behaviour of the material during crack propagation. The present work tries to characterize the behaviour of particleboard after a crack has formed and its propagation. To achieve this, energy considerations are applied.

One way is to measure the whole energy that is necessary to split a specimen (fracture energy concept, Nakayama 1965) under steady state crack propagation to obtain the specific fracture energy G_f. The specific fracture energy characterizes the energy which is necessary to create a unit area of new fracture surface. Especially for heterogeneous

Received 5 September 1995

Robert J. A. Ehart, Elmar K. Tschegg
Institute of Applied and Technical Physics
Technical University of Vienna
Karlsplatz 13, A 1040 Wien, Austria

Stefanie E. Stanzl-Tschegg
Institute of Meteorology and Physics
University of Agriculture of Vienna
Türkenschanzstraße 18, A 1180 Wien, Austria

The authors thank Dr. D. M. Tan for conducting the FE-calculations. Financial support by the Fonds zur Förderung der wissenschaftlichen Forschung, Wien is gratefully acknowledged

materials with a large crack tip process zone, G_f depends on the specimen size (size-effect) (Bazant 1984; Aicher 1993). The reason for this is that the size of the process-zone exceeds the remaining ligament length as the crack tip approaches the edge of the ligament. Therefore the fracture energy is reduced by that part of energy that is consumed to form the process zone. The size-effect is negligible only if the ligament length is sufficiently large.

More detailed information on the energy balance during crack propagation can be obtained from the crack-resistance concept. To determine the crack resistance the supplied energy, which causes crack propagation and crack length increment have to be measured simultaneously. The load-displacement curves contain information about the energy balance of the testing system but direct measurement of the crack length is not possible with sufficient accuracy because of the coarse structure of the investigated material. In addition a clear definition of the crack tip is difficult. This fact is caused by the different fracture mechanisms being effective. Microcracking in the frontal process-zone begins to reduce the strength of the material, but complete failure does not occur even behind the crack tip, as the crack surfaces are still bridged by fibers (Fig. 1). Furthermore, a characterization of the crack length by means of the electric resistance is impossible because of the low electric conductivity of the material. However, information about the crack length can be obtained indirectly from the load-displacement curves by the compliance of the specimen, if several unloading-reloading cycles are carried out after a small crack increment (compliance method). Especially for composites of stiff fibers, however, the unloading and reloading process is accompanied by friction- and interlocking effects, so that the application of this method is complicated for particleboard.

The method of Sakai and Bradt (1986) avoids unloading-reloading cycles and records the load-displacement curves for several specimens with different notch depths. For a linear elastic, brittle material these curves begin as straight lines with different slopes, according to the different compliances. The decreasing branches of these curves coincide after crack initiation, as the specimens with deeper notches do not differ from the others once the crack has reached the same length. For materials with pronounced plastic deformation, the curves of specimens with the shortest notches are stretched along the displacement axis so that the other curves have to be shifted to the right to attain coincidence. For fiber composites, however, there is a difference between cracked and notched specimens because of the bridging zone behind the crack tip (Fig. 2). A modification of this idea, however, would allow this method to be applied to such

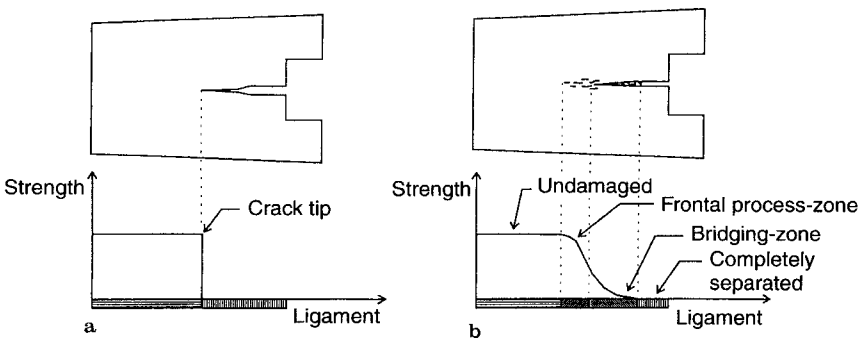

Fig. 1a and b. Damage of the material in the ligament. **a** Brittle material, **b** heterogeneous material with microcracking and bridging as fracture mechanisms

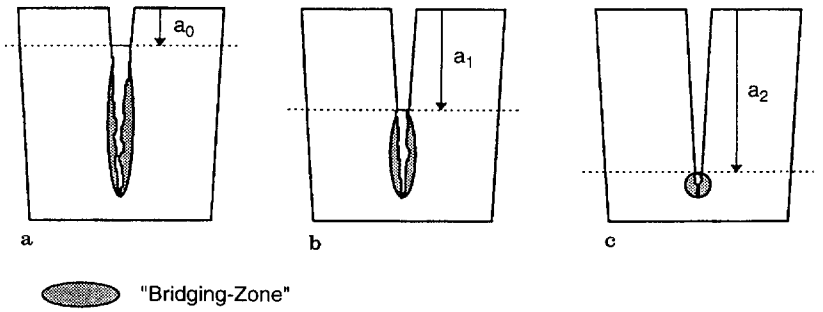

Fig. 2a–c. Different lengths of the bridging-zones for specimens with different notch-depths a_0, a_1, a_2, but identical total crack length

materials (see chapter evaluation). Nevertheless, it is difficult to apply this method to wood and wood composites, as wood is an extremely inhomogeneous material and load-displacement-curves for different specimens have to be compared. Therefore a large number of specimens has to be tested, owing to the large scatter of the data.

The evaluation method used in this paper (dimensionless load-displacement curves; Sakai and Inagaki 1989) derives the crack resistance by comparison of the measured load-displacement curves with the one calculated for the same specimen geometry under the assumption of linear elastic material behaviour. Taking care of the heterogeneous structure of particleboard, a material specific modification of the evaluation method concerning the unloading behaviour of particleboard was made. This material model together with the one introduced by Sakai gives two limits for the actual material behaviour during crack propagation. The calculations are described in chapter 3.

Experiments

Experimental device

To determine the fracture properties of the investigated material the wedge splitting method according to Tschegg (1986) was used. With this method, a vertical force is applied to a notched specimen (Fig. 3) by the testing machine. This force is transferred into the splitting force (Mode I loading) by a wedge and force transmission pieces which are placed into an appropriate groove of the specimen. To reduce friction between wedge and load transmission pieces roll-bodies are placed between them. The splitting force can be calculated from the vertical force and the wedge-angle. This method allows steady state crack propagation, the ratio of specimen volume to fracture surface area is very low (which is advantageous) and specimen preparation does not demand high efforts.

Specimen geometry and design of the loading device allow measurement under the condition of steady state crack propagation. This means that the crack is driven by the externally applied load and crack propagation can be stopped at any time by reducing this load. The released strain energy may never exceed the energy that is necessary to cause a crack-length increment. The energy balance of the testing system can be written as (Menz and Schlaich 1984)

$$-dU + dW = d\Gamma \tag{1}$$

with the work done by the machine dW, the potential energy change dU and the energy $d\Gamma$ consumed for crack growth.

Main part of the work done by the external load is stored elastically in the specimen at the begin of crack propagation, but this is released as the tension forces in the specimen are reduced during crack extension. As soon as the released strain energy equals the energy that is necessary for crack extension, the crack is driven only by the released strain energy ($dW = 0$).

$$-dU = d\Gamma \tag{2}$$

In this stage the change of these two energies with increasing crack length determines the further stability of crack growth. The condition for steady state crack propagation becomes

$$-\frac{dU}{da} \leq \frac{d\Gamma}{da}. \tag{3}$$

The measurements of this study have been carried out under crosshead speed control with a crosshead speed of 2.0 mm/min with a half wedge angle of 15°. Applied load and crack mouth opening displacement CMOD were measured with a load cell and two LVDTs fixed to the specimen with a special frame on the front and back side of the specimen. Two LVDTs were used in order to prove the symmetry of crack propagation. The frame allows the CMOD to be measured at the point where the load is applied. As it is fixed to the specimen near the crack tip, deformations and crack initiations near the loading device are excluded from measurement. The current values of load and CMOD were registered by the software system DIA/DAGO, so that the results of the measurement are load-displacement curves which can be used for further calculations.

Specimen size and geometry

The experiments were carried out for two different orientations, one with the notch plane (= plane of the crack surface) perpendicular to the board plane (Fig. 3a). In order to study the internal bonding of the used particleboard, tests were also performed with specimens with the notch plane parallel to the board plane. To allow testing in this orientation three plates were glued together (Fig. 3b). Although these specimens have a low ratio of width to length, which might cause instability during crack propagation for homogenous brittle materials, such problems are not to be expected as the side and the middle plates are subjected to different loading cases. The middle plate is subjected

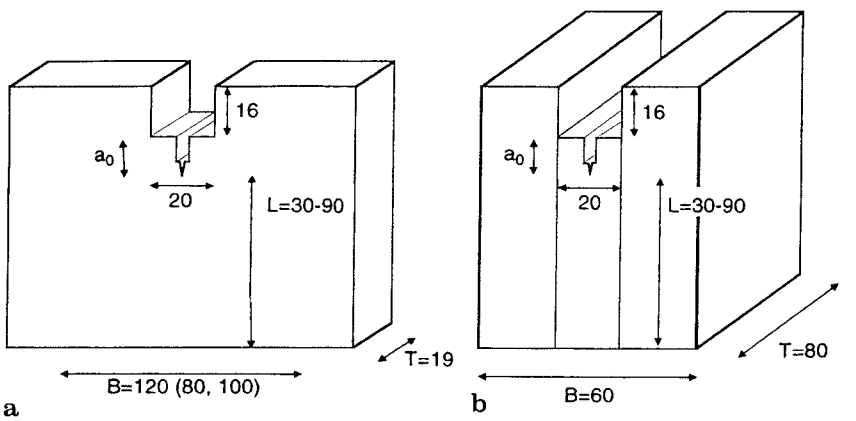

Fig. 3a and b. Specimen geometry with crack surface. **a** Perpendicular to the board-plane and **b** parallel to the board plane (dimensions in mm)

to Mode I-loading, for which mode the material has the lowest strength, whereas the outer plates are just subjected to bending.

To investigate the influence of specimen size and geometry, specimens with different notch depths a_0, different ligament lengths L and width B have been tested. Table 1 and Fig. 3 show the geometry for the different test series with different orientations of the notch plane to the panel plane.

Evaluation

One important fracture property of some material is the specific fracture energy G_f. It can be determined from the load-displacement curves recorded during steady state crack propagation as the area under the load-displacement curve, which is the total work done by the machine. Division by the ligament area yields the specific fracture energy G_f.

$$G_f = \frac{1}{A_{lig}} \int_0^{CMOD_{max}} F(CMOD)\, d(CMOD) \tag{4}$$

For materials with a large crack tip process zone the specific fracture energy depends on the specimen size, as no process zone can be formed any more when the process zone approaches the edge of the specimen (size-effect). Therefore the energy consumed by this process zone is missing.

The specific fracture energy is a mean value of the energy consumed by all small crack increments during crack propagation. A more detailed characterization of the material behaviour is achieved by the concept of the crack resistance curves. The crack resistance R_C is the energy needed to create a unit of new fracture surface. It may vary for different stages of crack propagation. These variations are caused by different fracture mechanisms such as microcracking in the frontal process zone and bridging in the wake of the crack tip. The size of these zones depends on the crack length. To determine R_C, simultaneous measurement of supplied energy and the resulting crack increment is necessary. As explained in chapter 1 the crack length cannot be determined experimentally with sufficient accuracy for the investigated material. Therefore graphical and numerical methods have been used.

For an evaluation according to the superposition method, load-displacement curves of specimens with different notch depths are compared. Especially for fiber composites a general coincidence of the decreasing branch cannot be achieved by shifting the curves, as specimens with different notch depths do not only differ as to the amount of their "plastic" deformations, but also as to the length of the bridging zone (Fig. 2). Nevertheless a coincidence should be possible at high crack lengths (large crack mouth opening displacements), when the length of the bridging zones have become equal (Fig. 4). This is possible as soon as the distance between the crack surfaces becomes larger than the length of the fibers and therefore bridging is no longer effective near the initial notch. In such stages there should be no difference (bridging zone) between the load-displacement curves of specimens with different notch depths. Load-displacement curves for specimens with crack plane parallel to the panel plane and notch depths of 10, 25, 40 and 55 mm are shown in Fig. 5. In Fig. 6 the shift to achieve coincidence for late stages of crack propagation has been carried out.

A main difficulty of this method is, that large errors can occur during shifting, caused by the fact, that load-displacement curves of different specimens with a large scatter of their mechanical properties have to be compared. Therefore another method was used for further evaluations in the present study.

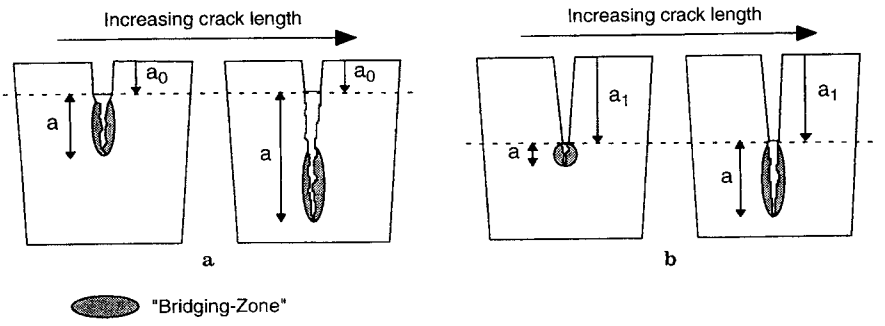

Fig. 4a and b. Although the lengths of the bridging-zones are different for specimens with different notch depths (a_0 for specimen (**a**) and a_1 for specimen (**b**)) at the beginning of crack formation, their lengths become equal in a later stage of crack propagation

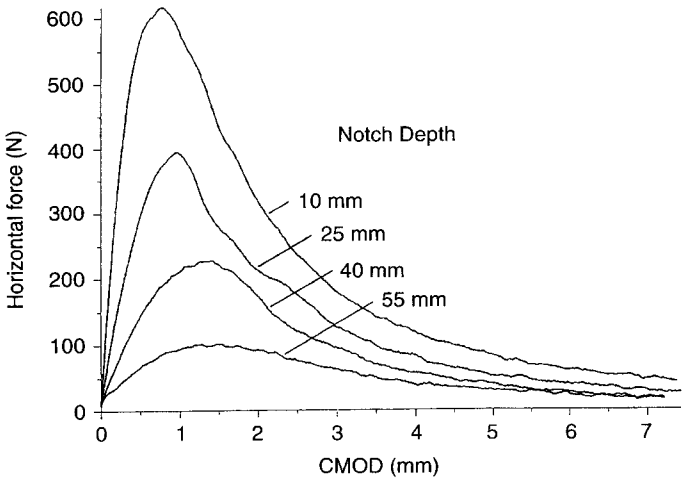

Fig. 5. Load-displacement curves for specimens with crack plane parallel to the board plane and different notch depths

The measured load-displacement curves have been evaluated similar to the so called method of the dimensionless load-displacement curves (Sakai and Bradt, 1986). For this, a theoretical load-displacement curve was calculated by means of FE-methods under the assumption of linear elastic material behaviour. For a linear elastic material the following equations describe the dependence of the critical stress-intensity factor K_{IC} and the loadpoint displacement on the crack length (Tschegg and Tan 1995)

$$K_{IC} = \frac{P_C}{2TL} f_k(a) \tag{5}$$

$$u = \frac{P}{ET} f_D(a), \tag{6}$$

where T and L are specimen thickness and length.

The functions $f_k(a)$ and $f_D(a)$ in Eqs. 5 and 6 were calculated by assuming a certain crack length a and calculating the J-integral for this configuration. The advantage of

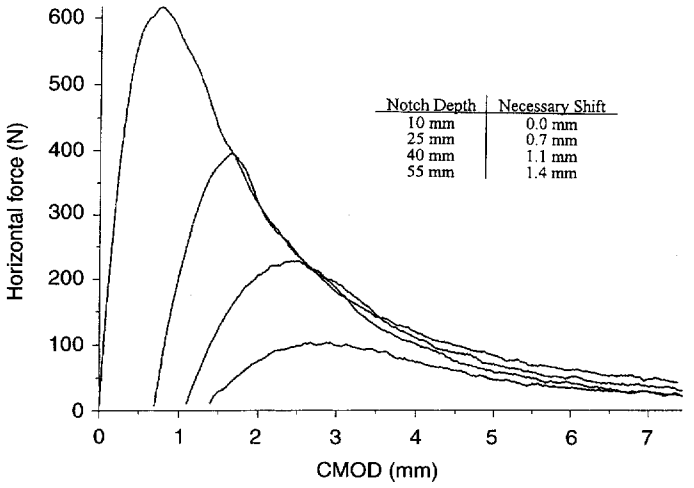

Fig. 6. Load-displacement curves of Fig. 5 after shifting them in horizontal direction in order to achieve coincidence of the decreasing part of the curves. The amount of necessary shift yields the difference of the plastic deformations having occurred during testing

using the J-integral (Rice 1968) is that its value does not depend on the shape of the contour on which it is calculated, as long as the contour encloses the crack tip so that areas with high stresses can be eluded. The J-integral is related to the K value by the relation

$$J = \frac{K^2}{E'} \tag{7}$$

which is correct for a linear elastic material.

For a given specimen geometry, the theoretical linear elastic load-displacement curve is characterized by the two parameters E′ (effective Young's modulus) and K_{IC} (critical stress-intensity factor). They can be used to "scale" the theoretical load-displacement curve to the measured one in such a way that correlated curves have the same initial slope and maximum force (Fig. 10). Using the slope of the beginning of the load-displacement curve, the Young's modulus E′ can be calculated using Eq. 6 without crack extension.

$$E' = \frac{P}{u} \frac{f_D(0)}{T} \tag{8}$$

The critical stress-intensity factor K_{IC} is derived from Eq. 5 assuming that crack propagation starts when the maximum load is applied. As the influence of crack length on the stress intensity factor is described by the function $f_D(a)$, the load-displacement curve and the correlation between crack length and displacement is completely described for the linear elastic brittle material.

The measured load-displacement curve is dilated along the displacement axis in comparison to the calculated one with their points being correlated by the same load (Fig. 7). This dilatation is caused by the nonlinear behaviour of the investigated material, the main reasons of which can be either plastic deformations or the formation of microcracks (strain softening) as described in Fig. 8.

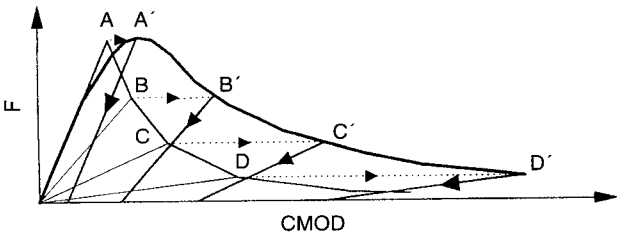

Fig. 7. Correlation (dashed lines) between points of the calculated load-displacement curve for a linear elastic material (A, B, C, D) and the measured one (A′, B′, C′, D′), which is dilated along the displacement axis because of nonlinear material behaviour. It is assumed, that the unloading paths (solid arrows) have the same slope for both, the linear elastic and the real material

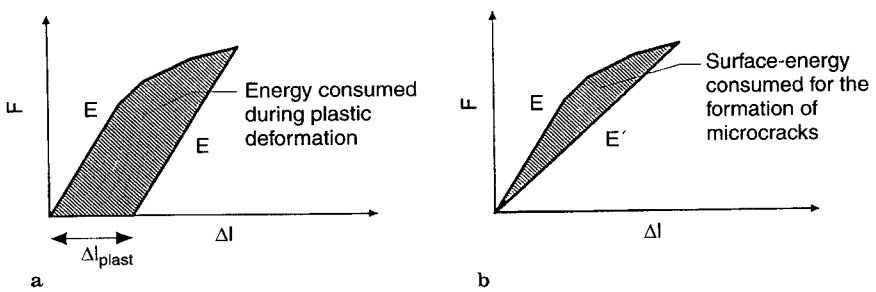

Fig. 8a and b. Different reasons for nonlinear material behaviour under tension. a Plastic deformation: If no hardening occurs, the same elastic modulus is valid for both, loading and unloading. b Strain softening: The formation of microcracks reduces the effective cross-section and the elastic modulus is reduced ($E' < E$)

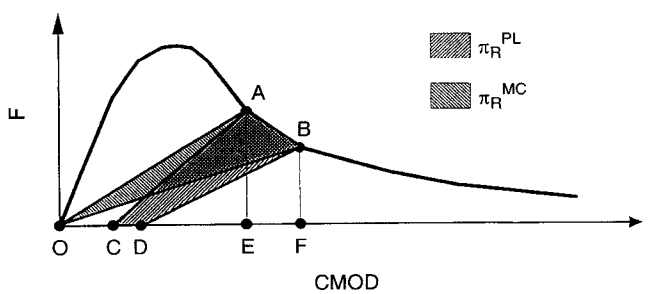

Fig. 9. Areas for the calculation of the fracture resistance for different material models. MC: microcracking as only reason for nonlinearity. PL: plastic deformations only. The stored elastic strain energy for different stages of crack propagation A and B corresponds to the areas ACE and BDF respectively for a plastic material. If no plastic deformations occur, the lines AC and BD would go back to the origin

If the additional displacement were caused by plastic deformations only (Fig. 8a), unloading of the specimen would result in a straight line with the same slope for both the linear elastic and the tested material; the released strain energy would be the same for both materials (Fig. 7). Therefore load and displacement of a point of the measured load-displacement curve can be related to the crack length a using Eqs. 5 and 6, and the energy release rate $\tilde{G}_C$ can be calculated (difference of area ACE and BDF in Fig. 9).

If, contrarily, the only reason for deviations from linear elastic material behaviour were the formation of microcracks in the crack tip process zone (strain softening), the unloading path would be a straight line going back to the origin, with a different compliance of the specimen (Fig. 8b). In this case the released strain energy is the difference of the areas OAE and OBF in Fig. 9.

The difference of supplied work dW (area ABFE in Fig. 9) and released energy is the energy used for crack propagation $d\Gamma$ (π_R area ABDC and OAB in Fig. 9). Division by the area of the created crack surface gives the crack resistance R_C.

$$R_{C,i} = \frac{\partial \pi_R}{\partial A_i} = \frac{\Delta \pi_R}{T(a_{i+1} - a_i)}, \tag{9}$$

where π_R is the area ABCD or ABO in Fig. 9, depending on which of the two models is assumed.

Correlation of points of the experimental and calculated load-displacement curves by the same force in Fig. 7, however, means that the determined crack length in the actual specimens is an effective crack length. A linear elastic material with a clearly defined crack tip and thus specified crack and remaining ligament length can transfer the same force as the remaining ligament of the tested specimen with crack tip process zone and bridging zone.

Results and discussion

Load-displacement curves

To investigate the influence of specimen size and geometry on the specific fracture energy, different specimen series have been tested for both orientations. According to Table 1 (crack surface perpendicular to the board plane), specimens of the first test series differ in ligament length only, with all other dimensions kept constant. In the next series a variation in notch depth was carried out with constant specimen length, and in a final test series specimens with different widths have been tested. The recorded load-displacement curves (Ehart 1994) indicate that their general shape is strongly influenced by the ratio of specimen length to width as long as the dimensions do not exceed defined minimum values. Especially for narrow specimens the side parts of the specimen are much more deformed (bended), so that the stress distribution in the ligament is changed. Therefore high stresses (Mode I) are restricted to a smaller part of the ligament in narrow specimens. So the load keeps its high value close to its maximum during crack propagation up to larger crack mouth opening displacements (CMOD's) (dashed and dotted curves in Fig. 10). Their maximum load is of course lower than the one of wider specimens (solid curve in Fig. 10). At larger CMOD's the load of narrow

Table 1. Orientation of the crack plane to the panel plane and specimen geometry for the tested specimens. *) This geometry was used for the R_C-calculations

Orientation	Test series	L [mm]	T [mm]	a_0 [mm]	B [mm]
Perpendicular	Ligament length	30, 45, 60, 75*, 90	19	10	120
Perpendicular	Notch depth	75	19	10*, 25, 40, 55	120
Perpendicular	Specimen width	75	19	10	80, 100
Parallel	Ligament length	30, 45, 60, 75, 90	80	10	59
Parallel	Notch depth	75	80	10, 25, 40, 55	59
Parallel	Specimen thickness	75	40, 60, 80	10	59

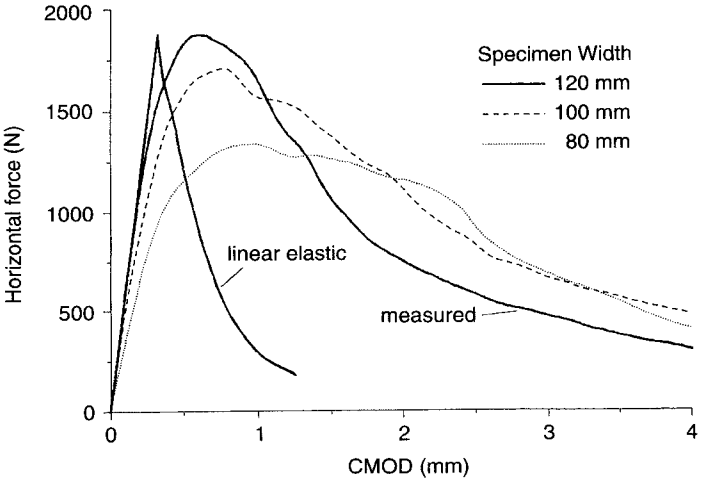

Fig. 10. Measured and calculated (linear elastic) load-displacement curves (solid lines) for a specimen with crack surface perpendicular to the panel plane, a ligament length of 75 mm and a specimen width of 120 mm. Dashed curve: typical measured curve for a specimen width B of 100 mm, Dotted curve: typical measured curve for a specimen width B of 80 mm

specimens remains even higher than the one of wide specimens, which decreases much stronger after the maximum load. The contribution of these parts of the load displacement curves to the specific fracture energy approximately compensates the lower energy consumption owing to the lower forces at the begin of loading. Therefore, apart from the scatter of data, no influence of specimen width on the specific fracture energy results within the tested width range.

Equivalent test series have been conducted with specimens with varying ligament length and varying notch depth for the orientation with the crack surface parallel to the panel plane. In addition, specimens with different thickness have been tested, revealing no significant dependence of the fracture properties on the specimen thickness.

Specific fracture energy, G_f

The specific fracture energy was calculated from the load-displacement curves by evaluating the total area enclosed by the curve and the load axis and division by the crack surface area. Comparing the specific fracture energies of specimens with different dimensions (Ehart 1994) and the crack surface perpendicular to the panel plane shows, that despite of the high scatter of the data a size-effect (about 20% of the specific fracture energy G_f, if the ligament length is reduced from 75 to 30 mm) can be noticed for the tested specimens. From the trend of the G_f values, a minimum ligament-length of 70 mm was found to be necessary to be able to neglect the influence of the ligament length on the specific fracture energy. A mean value of G_f of 2930 N/m for specimens with ligament length of at least 75 mm was found for this orientation.

For specimens with the crack surface parallel to the panel plane, a G_f value of 240 N/m with a size effect of 27% for the same ligament lengths as above was determined. This result demonstrates, that the fracture properties of particleboard differ by a factor of approximately 10 for the different orientations.

Crack resistance curves

The crack resistance curves have been determined according to Fig. 9 (Area ABCD). For this an ideal load-displacement curve was calculated by FE-methods. This curve can be "scaled" to the experimentally recorded load-displacement curves by choosing the Young's modulus and the critical stress intensity factor in a way, that both curves have the same initial slope and maximum load (solid lines in Fig. 10). Using the first model ("plastic model") the dilatation of the measured load-displacement curve compared to the theoretical one is interpreted as a consequence of plastic deformations only, and therefore the same slope of the unloading path from points of both curves is assumed. From the theoretical load-displacement curve the energy release rate and the crack length can be calculated. As points of the two curves are correlated by the same load, the determined crack length has to be regarded as an effective crack length, for which the ligament of a linear elastic brittle specimen can transmit the same force.

The crack resistance curves R_C^{PL} of specimens with the fracture surface perpendicular to the panel-plane are shown in Fig. 11. The results indicate fluctuations of R_C^{PL} in a range of $\pm 25\%$ of the specific fracture energy G_f and over a typical length of 10 mm as a consequence of inhomogeneities of the material. The solid curve in Fig. 11 was obtained by a regression analysis as a third degree polynom and represents the mean R_C^{PL} values for specified crack lengths. This curve first decreases and has a minimum at a crack length of about 20 mm. This seems to be caused by crack initiation processes, where at the begin energy is consumed to sharpen the notch and create the crack tip process zone. After the minimum, the mean crack resistance increases with increasing crack length up to a crack length of approximately 45 mm. The increase may be explained by the size of the bridging zone, which is still growing at this stage of crack propagation. For larger crack lengths, the R_C^{PL} values remain constant or begin to decrease slightly. This can be explained by the fact, that the length of the bridging zone starts to decrease as an effect of the limited specimen size.

If the crack surface is parallel to the panel-plane, a similar behaviour is observed (no figure included), with a much smaller increase of the curves after the minimum. This result is explained by the preferential fiber orientation being parallel to the crack surface thus causing lower bridging forces behind the crack tip.

Besides R_C^{PL}, the energy release $\tilde{G}_C^{PL}$ is plotted in Fig. 11. $\tilde{G}_C^{PL}$ was calculated as the difference of the areas ACE and BDF in Fig. 9 divided by the increment of the crack surface area. The small contribution of the energy release rate to the crack resistance indicates that crack propagation indeed was predominantly stable. At the begin of crack growth, $\tilde{G}_C^{PL}$ is very low and even negative, as elastic energy is stored in the specimen. Later, $\tilde{G}_C^{PL}$ remains positive, indicating that the stored elastic energy is released as the stress in the specimen is reduced. The energy release rate $\tilde{G}_C^{PL}$ is almost the same for all specimens, as it is derived from the calculated load-displacement curve for a linear elastic material, which was scaled to the maximum force of the measured curve as described in chapter 3.

As a reference line also the specific fracture energy G_f and the crack initiation energy γ_{ini} divided by the crack surface area are plotted in Fig. 11.

Guided by the heterogeneous structure of particleboard, the crack resistance curves have been evaluated alternatively with another material model, in which formation of microcracks is assumed to be the only reason for deviations from linear elastic material behaviour. Consequently it is assumed, that the unloading paths from points of the experimental load-displacement curve go back to the origin (see Fig. 8b), causing an energy release rate $\tilde{G}_C^{MC}$ different from that of the "plastic model". In this case the crack resistance curves (Fig. 12) show similar behaviour to the ones calculated according to the "plastic model". The energy release rate, however, becomes more important for the

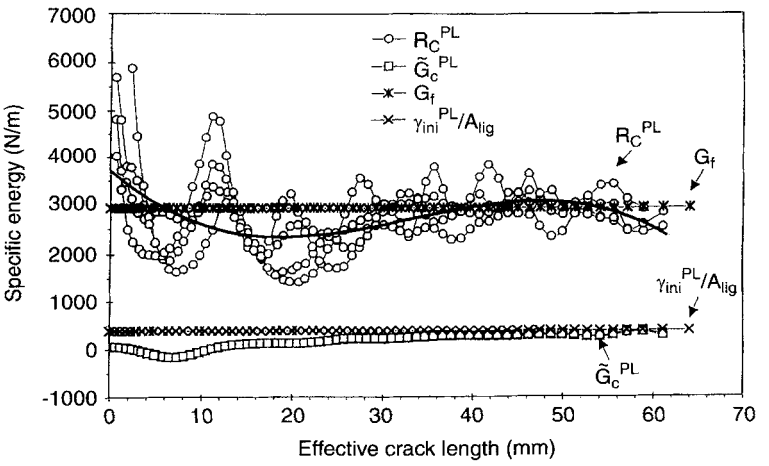

Fig. 11. Crack resistance R_C^{PL} and released strain energy $\tilde{G}_C^{PL}$ for four different specimens of the same geometry with the crack plane perpendicular to the board plane, assuming that plastic deformations are the only reason for deviations from linear elastic material behaviour. Specific fracture energy G_f and crack initiation energy γ_{ini}^{PL} divided by the crack surface area are plotted as reference lines

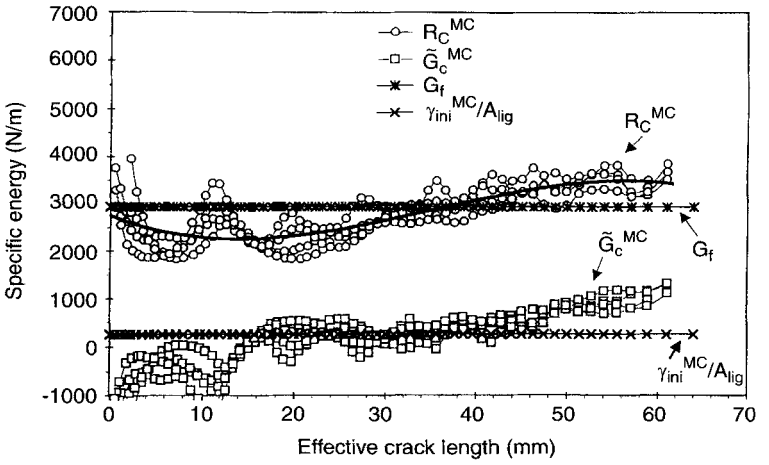

Fig. 12. Crack resistance R_C^{MC} and released strain energy $\tilde{G}_C^{MC}$ for four different specimens of the same geometry with crack plane perpendicular to the board plane and assuming that the formation of microcracks is the only reason for deviations from linear elastic material behaviour. Specific fracture energy and crack initiation energy are plotted as reference lines

energy balance of crack propagation as microcracking lowers the effective Young's modulus of the material and therefore more elastic energy is stored. An increase of the crack resistance is accompanied by a higher supply of elastic energy into the specimen so that the oscillations of $\tilde{G}_C^{MC}$ look mirrored to those of R_C^{MC}.

The actual material behaviour is expected to be a combination of these two ideal material models, which serve as extreme cases.

Crack initiation energy

For both models it is assumed that crack propagation begins, when the maximum force is applied. Actually microcracking processes take place earlier – at the beginning of deviations from linear elastic behaviour. Therefore the energy consumed for the formation of this notch tip process zone (crack initiation energy γ_{ini}) is not included in the calculated crack resistance and was determined separately as the difference of the work supplied by the machine until the maximum load is reached and the calculated linear elastic strain energy for the maximum load according to

$$\gamma_{ini}^{PL} = \int_0^{u_{max}} F(u)\,du - \frac{1}{2} F_{max} u_{max}^{th} \tag{10}$$

and Fig. 13. Table 2 contains the results of the calculations. The crack initiation energy γ_{ini}^{PL} is 13% of the total fracture energy for the "plastic model", which allows a simple estimation of the length of the crack tip process zone of about 10 mm. If the evaluation is carried out according to the strain softening model (microcracking) using Eq. 10 but substituting u_{max}^{th} (the theoretical displacement at maximum load) by u_{max} (the experimentally determined displacement at maximum load), the share of the crack initiation energy γ_{ini}^{MC} is 6% of the total fracture energy. From this the length of the crack tip process zone is estimated to be 5 mm.

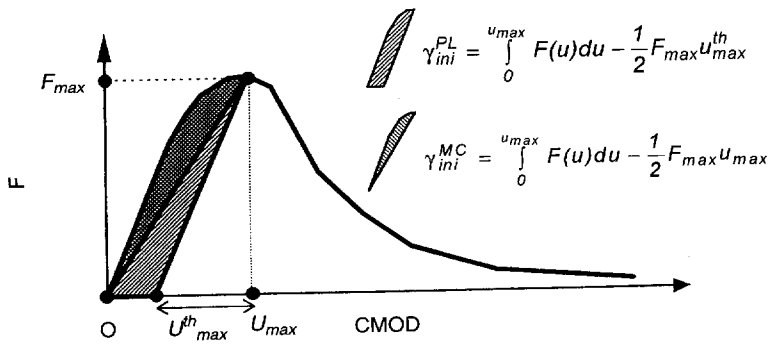

Fig. 13. Calculation of the crack initiation energy γ_{ini}^{PL} according to the "plastic model", where the same slope at the beginning of loading and for unloading is assumed. If the "microcracking-model" is applied (γ_{ini}^{MC}), the unloading path from the maximum load goes back to the origin

Table 2. Results of the splitting tests for identical specimens with crack plane perpendicular to the panel plane and a ligament length of 75 mm

Specimen	G_f [N/m]	γ_{ini}^{PL} [N mm]	E [N/mm^2]	K_{IC} [N/mm^{1,5}]	γ_{ini}^{MC}
A	2898,13	468	5552	44,79	207
B	2936,62	544	5042	41,28	251
C	3055,6	622	4573	38,93	281
D	2832,13	597	4783	41,15	270
Mean value	2930,62	557,75	4987,5	41,54	252,25
Stddev	93,8	68,1	422,4	2,42	32,6
Rel. dev.	3,2%	12,2%	8,5%	5,8%	12,9%

Summary and conclusion

Aim of this work was to characterize and quantify crack propagation in particleboard. For this, splitting tests according to Tschegg (1986) have been carried out. It is shown that this method can be applied successfully to specimens of particleboard and allows testing under steady state crack propagation. The results of the tests are load-displacement curves, which can be used to characterize the fracture properties of the investigated material. From the load-displacement curves several fracture properties can be determined directly, such as the specific fracture energy G_f, the maximum load and the crack initiation energy γ_{ini}.

For specimens with crack surface perpendicular to the panel plane a mean value of the specific fracture energy G_f of 2930 N/m was found, with a share of crack initiation energy γ_{ini} of 6 to 13% (252 to 558 N mm), depending on the material model used. From this, a simple estimation of the size of the crack tip process zone gives an approximate length of 5 to 10 mm. Crack propagation parallel to the panel plane yields a specific fracture energy of 240 N/m, which is less than 10% of that in the perpendicular direction.

As the concepts of LEFM do not seem to be appropriate to characterize particleboard, energy based concepts have been used to describe crack propagation processes by means of the crack resistance R_C. To evaluate R_C an application of the superposition method turned out to be difficult, which was mainly due to the inhomogeneity of the material.

The so-called method of dimensionless load-displacement curves (Sakai and Bradt 1986) avoids a direct measurement of crack length and allows an evaluation with single specimens, using the measured as well as the load-displacement curve of a linear elastic brittle material. This curve was calculated by FE-methods. For the evaluation the measured load-displacement curves and two different material models have been used in the present study.

For the first model, plastic deformations and for the second one, formation of microcracks (strain softening) were assumed to be the only reason for nonlinear material behaviour. The resulting crack resistance curves of the two models (Figs. 11, 12) indicate fluctuations of R_C up to 25% of the specific fracture energy, which result from material inhomogeneities. The overall mean value curve increases slightly with increasing crack length up to a crack length of 45 mm, which indicates, that the length of the bridging zone increases up to this crack length. For further crack extension R_C remains constant or starts to decrease as an effect of the limited specimen size.

The calculated crack resistance curves give detailed information on crack propagation in particleboard, as their behaviour is a consequence of the size of the bridging- and the frontal process-zone and they also contain information on the extent of material inhomogeneities. Accordingly they can be used to investigate the influence of several production parameters, such as particle size, glue and kind of wood, as well as the influence of environmental conditions (temperature, air humidity, . . .) on the fracture behaviour and therefore the quality of particleboard. In addition, the presented evaluation procedures can be successfully used to characterize any other non-linear material, like solid wood.

Additional experiments to characterize the middle and outer layers of inhomogeneous boards separately are in preparation.

References

Aicher, S.; Reinhardt, H. W. 1993: Einfluß der Bauteilgröße in der linearen und nichtlinearen (Holz-)Bruchmechanik. Holz Roh- Werkstoff 51: 215–220

Bazant, Z. P. 1984: Size effect in blunt fracture: Concrete, rock, metal. J. of Engineering Mechanics 110 (4): 518–535
Ehart, R. J. A. 1994: Charakterisierung des Bruchverhaltens von Holzfaserverbundwerkstoffen – Experimente. Modellierung und FE-Simulationen. Master Thesis, Technical University of Vienna
Menz, W.; Schlaich, J. 1984: Rißwiderstand und Rißfortschritt bei Glasfaserbeton. In: Ellinghausen, R.; Rußwurm, D. (Ed.): Fortschritte im konstruktiven Ingenieurbau. pp. 207–219. Berlin: Verlag für Architektur und technische Wissenschaften
Nakayama, J. 1965: Direct measurement of fracture energies of brittle heterogeneous materials. J. Am. Ceram. Soc. 48(11): 583–587
Niemz, P.; Schädlich, S. 1992: Untersuchungen zum Einfluß der Struktur auf die Bruchzähigkeit von Spanplatten: Holz Roh- Werkstoff 50: 389–391
Rice, J. R. 1968: A path independent integral and the approximate analysis of strain concentrations by notches and cracks. J. Appl. Mech. 35: 379–386
Sakai, M.; Bradt, R. C. 1986: Graphical methods for determining the nonlinear fracture parameters of silica and graphite refractory composites. In: Bradt, R. C.; Evans, A. G. (Ed.): Fract. Mech. of Ceram. 7: 127–142. New York-London: Plenum Press
Sakai, M.; Inagaki, M. 1989: Dimensionless load-displacement relation and its application to crack propagation problems. J. Am. Ceram. Soc. 72(3): 388–394
Tschegg, E. K. 1986: Equipment and appropriate specimen shapes for tests to measure fracture values (in German). Patent No. 390328, 1986, Österreichisches Patentamt
Tschegg, S.; Tan, D. M.; Tschegg, E. K. 1996: Fracture resistance of crack propagation in wood. Int. J. of Fracture, accepted 1996